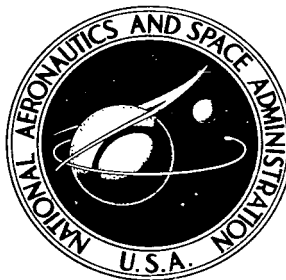


NASA TECHNICAL NOTE



NASA TN D-6019

C.1

NASA TN D-6019

LOAN COPY: RETURN  
AFWL (DOGL)  
KIRTLAND AFB, N. M.

0132669



TECH LIBRARY KAFB, NM

COUPLED SUPERSONIC INLET-ENGINE  
CONTROL USING OVERBOARD BYPASS DOORS  
AND ENGINE SPEED TO CONTROL  
NORMAL SHOCK POSITION

*by Gary L. Cole, George H. Neiner,  
and Robert E. Wallhagen*

*Lewis Research Center  
Cleveland, Ohio 44135*

NATIONAL AERONAUTICS AND SPACE ADMINISTRATION • WASHINGTON, D. C. • DECEMBER 1970



0132669

1. Report No. NASA TN D-6019		2. Government Accession No.		3. Acquisition Statement	
4. Title and Subtitle COUPLED SUPERSONIC INLET-ENGINE CONTROL USING OVERBOARD BYPASS DOORS AND ENGINE SPEED TO CONTROL NORMAL SHOCK POSITION				5. Report Date December 1970	
7. Author(s) Gary L. Cole, George H. Neiner, and Robert E. Wallhagen				6. Performing Organization Code	
9. Performing Organization Name and Address Lewis Research Center National Aeronautics and Space Administration Cleveland, Ohio 44135				8. Performing Organization Report No. E-5499	
12. Sponsoring Agency Name and Address National Aeronautics and Space Administration Washington, D. C. 20546				10. Work Unit No. 720-03	
15. Supplementary Notes				11. Contract or Grant No.	
16. Abstract  An inlet normal shock control was investigated which used the inlet's high response by-pass doors as the primary manipulated variable and engine speed as a slow-acting re-set control. One advantage of this control concept over separate inlet and engine controls is that it allows the inlet's overboard bypass system to be operated at the most efficient position. Another advantage is that this control can correct for shock displacements in the aft direction when the bypass doors are initially closed. A separate inlet control cannot. Experimental results show that the control operates satisfactorily, returning the inlet quickly to design conditions, when subjected to disturbances in diffuser exit corrected airflow.				13. Type of Report and Period Covered Technical Note	
17. Key Words (Suggested by Author(s)) Normal shock control Propulsion system control Supersonic inlet-engine control				14. Sponsoring Agency Code	
18. Distribution Statement  Unclassified - unlimited					
19. Security Classif. (of this report) Unclassified	20. Security Classif. (of this page) Unclassified	21. No. of Pages 36	22. Price* \$3.00		

# COUPLED SUPERSONIC INLET-ENGINE CONTROL USING OVERBOARD BYPASS DOORS AND ENGINE SPEED TO CONTROL NORMAL SHOCK POSITION

by Gary L. Cole, George H. Neiner, and Robert E. Wallhagen

Lewis Research Center

## SUMMARY

A cross-coupled inlet-engine control concept was investigated for a supersonic propulsion system consisting of a mixed-compression inlet and a turbojet engine. The control system manipulates both bypass door flow area and engine speed to stabilize normal shock position in the inlet. The fast inlet overboard bypass door loop is the primary means of shock position control, and the engine speed loop is used as a slow-acting reset control. One advantage of this control concept is that the inlet's overboard bypass doors can be positioned such that the combination of overboard bypass drag and engine operating condition results in the most efficient propulsion system operation. This is accomplished by using engine speed to reset the bypass doors after they have been manipulated by the normal shock controller. Another advantage is that the coupled controls can correct for normal shock displacements in the aft direction even when the bypass doors are initially closed. A separate overboard bypass door loop could not make such a correction.

Experimental results are presented which show the performance of the separate inlet and engine controls as well as the coupled control system. The coupled control is shown to operate satisfactorily, returning the inlet quickly to design conditions, for step disturbances in diffuser exit corrected airflow. The propulsion system that was tested consisted of a NASA designed mixed-compression inlet coupled to a single rotor turbojet engine in the 18 000-newtons (4000-lb) thrust class. The propulsion system was operated at a Mach number of 2.5 in the Lewis 10- by 10-Foot Supersonic Wind Tunnel.

## INTRODUCTION

The payload that can be delivered by an aircraft is sensitive to the performance or efficiency of its propulsion system. In particular, the future of a commercial aircraft such as the supersonic transport depends on how economically the payload can be delivered.

Two variables that effect propulsion system efficiency are pressure recovery at the compressor face and drag due to spillage of excess airflow. The relative effects of these and other inlet variables on the payload of a typical supersonic transport configuration are indicated in reference 1.

In a mixed compression inlet, pressure recovery generally increases and airflow distortion decreases at the compressor face as the normal shock is moved closer to the aerodynamic throat. Thus, it is desirable for the shock operating point to be near the throat. However, disturbances can cause the shock to move from its operating point. A displacement in the upstream direction could result in an inlet unstart. A displacement in the downstream direction generally results in lower pressure recovery and higher distortion which might cause the compressor to stall. These events are undesirable and can be avoided in most cases by supplying the inlet with a normal shock control.

Control systems for mixed compression inlets have been investigated which manipulate the centerbody and overboard bypass doors near the diffuser exit to stabilize the normal shock position. Reference 2 describes normal shock controls which used high response bypass doors as the manipulated variable. Reference 3 describes a complete control system concept for a mixed compression inlet.

To date it has been conventional for the inlet and engine controls to function independently. However, the match of airflow between inlet and engine is affected by engine speed as well as bypass door position. Thus, by manipulating engine fuel flow to change engine speed, the bypass doors can be repositioned (if desired) after making the initial correction for a disturbance induced shock motion. The doors would be repositioned to reduce overboard bypass drag which could result in higher overall propulsion system efficiency. Cross coupling the controlled inlet and engine can, therefore, present significant advantages. The idea of coupling inlet and engine controls for stabilization of normal shock position has also been suggested in reference 4.

One example of a cross-coupled propulsion system control is to make use of engine speed as the fast acting control variable. In this case engine speed is rapidly changed to control shock position and the bypass doors are then moved to reset engine speed to its initial commanded value. This control technique was investigated experimentally and is documented in a companion report (ref. 5).

A second cross-coupled scheme uses fast acting bypass doors in conjunction with a slow reset action of engine speed. Thus engine speed is used as a slow reset to return the doors to their most efficient operating position. To demonstrate the feasibility of this second type of coupled inlet-engine control system, a program was conducted in the Lewis 10- by 10-Foot Supersonic Wind Tunnel using a mixed-compression inlet designed for Mach 2.5 and a J85-13 turbojet engine.

This report describes in the following order (1) the experimental setup and procedure, (2) the development of the individual controls - both the inlet normal shock control and the engine speed control, (3) the way in which the two control loops are coupled, and (4) the coupled control action and dynamics. Experimental results are presented and discussed.

## APPARATUS AND PROCEDURE

Testing of the normal shock control, speed control, and the cross-coupled control was conducted in the Lewis 10- by 10-Foot Supersonic Wind Tunnel. The propulsion system was composed of a mixed-compression inlet coupled to a single rotor turbojet engine. All tests were conducted at the following average free stream conditions: Mach number, 2.5; total temperature, 297 K; total pressure, 9.5 newtons per square centimeter; Reynolds number,  $4.5 \times 10^6$  (based on the cowl lip diameter); and specific heat ratio, 1.4. The propulsion system was operated at zero angle of attack during all tests. The engine operating speed during the tests was in the range of 87 to 90 percent mechanical speed or 86 to 88 percent corrected speed.

### Description of Inlet

The inlet, which was designed by NASA, is shown schematically in figure 1. The inlet was an axisymmetric, mixed-compression type with 60 percent of the supersonic area contraction occurring internally at its design Mach number of 2.5. The inlet had a cowl lip diameter of 47.3 centimeters, corresponding to a capture flow area of 1760 square centimeters.

Porous bleed regions forward of the inlet geometric throat and vortex generators in the subsonic diffuser were located on both the cowl and centerbody surfaces (as shown in fig. 1). The bleed regions were used for boundary layer bleed and to improve the inlet's stability characteristics. Vortex generators were used to decrease distortion of the pressure profile at the diffuser exit. Additional aerodynamic design details and steady-state performance characteristics of the inlet are given in references 6 and 7.

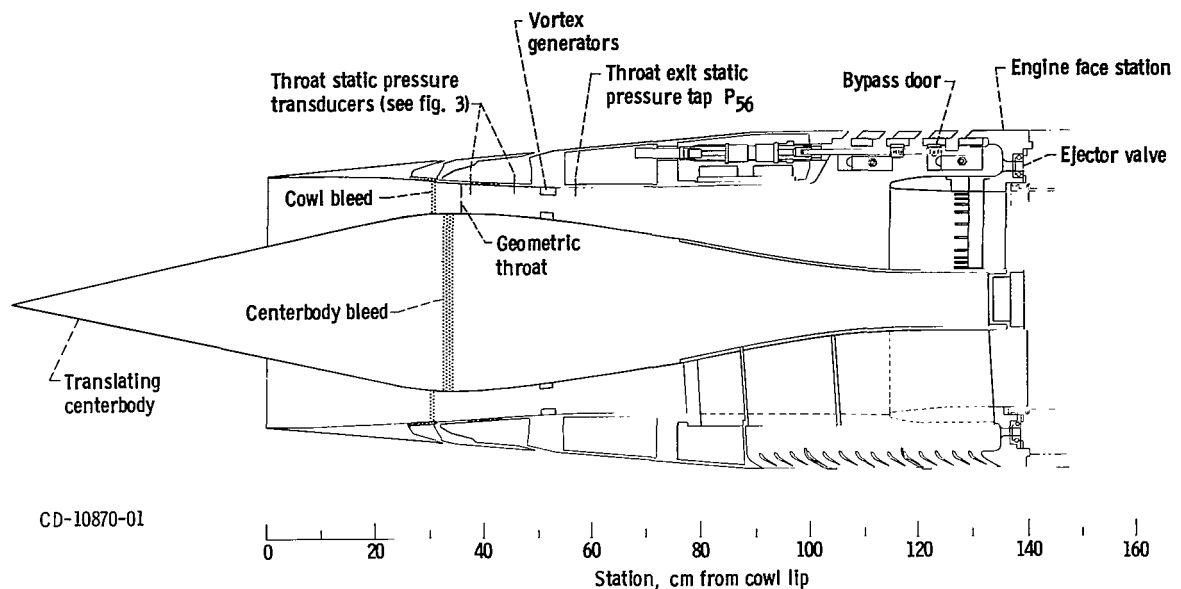


Figure 1. - Inlet details.

The dynamic response of the inlet's normal shock and various internal pressures to external and internal airflow disturbances is reported in reference 8.

The inlet had the following variable geometry features (shown in fig. 1): a translating centerbody, ejector valve, and six sliding plate overboard bypass doors. The centerbody was kept at its Mach 2.5 design position during the test program. The ejector valve, located at the diffuser exit, was used to supply cooling air to the engine (approximately 3 percent of total inlet airflow). The ejector and each bypass door exit was choked. The bypass doors were located symmetrically about the inlet just upstream of the diffuser exit and were used to match inlet airflow to engine airflow requirements. Each bypass door was hydraulically actuated and electronically controlled by an independent servochannel. Three symmetrically located doors, driven in parallel, were used to provide step and sinusoidal disturbances in diffuser exit corrected airflow. The remaining three doors, also driven in parallel, were used as the manipulated variable of the normal shock controller. The frequency response of the bypass doors, shown in figure 2, was flat within 0 to -3 decibels from 0 to 110 hertz. The response was taken for a commanded zero-to-peak amplitude of 7 percent of full travel. This amplitude was about the same as the disturbance amplitude used during frequency response tests of the inlet normal shock control and transient tests of the cross-coupled control. Additional details of the bypass door design and servoamplifier can be found in references 7 and 9, respectively.

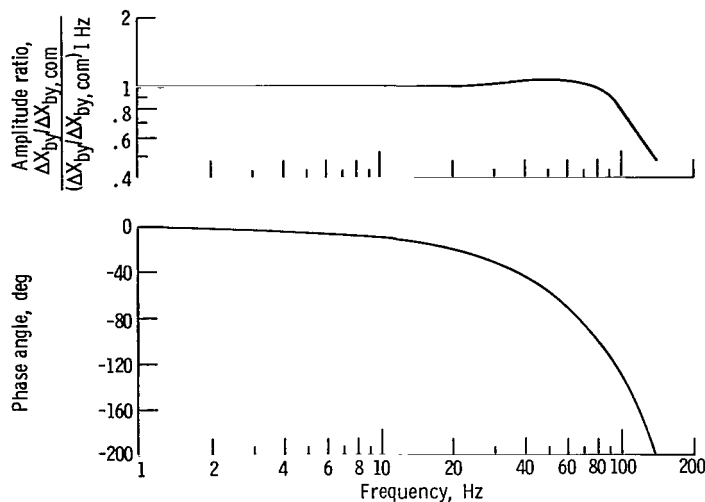


Figure 2. - Response of bypass door displacement to command in displacement. Zero-to-peak amplitude of command, 7 percent of full stroke.

## Inlet Instrumentation

The normal shock control used a throat exit static pressure  $P_{56}$  as the feedback variable. (Symbols defined in the appendix.)  $P_{56}$  was used instead of shock position primarily because it is easier to measure. Also, data from reference 8 show that the amplitude ratios of  $P_{56}$  and shock position to a diffuser exit airflow disturbance agree within 0 to 3 decibels over the frequency range from 0 to 90 hertz. Thus,  $P_{56}$  can be used as a good indicator of shock position for downstream disturbances. The performance of the normal shock control will be indicated in the test results section by traces of  $P_{56}$ .

The  $P_{56}$  static pressure tap was located 56.13 centimeters from the inlet cowl lip as shown in figures 1 and 3. The  $P_{56}$  tap was closely coupled to a dc strain-gage-type pressure transducer. The transducer and its coupled tubing had a frequency response that was flat within 0 to 2 decibels from 0 to 250 hertz for the amplitudes to which it was subjected during these tests.

## Shock Position Determination

Although  $P_{56}$  was used as the feedback variable for the normal shock control, it was desirable to know what the disturbance induced shock displacements actually were. The determination of normal shock displacement was aided by the use of static pressures a to h (shown in fig. 3). The taps for these pressures were located within the throat

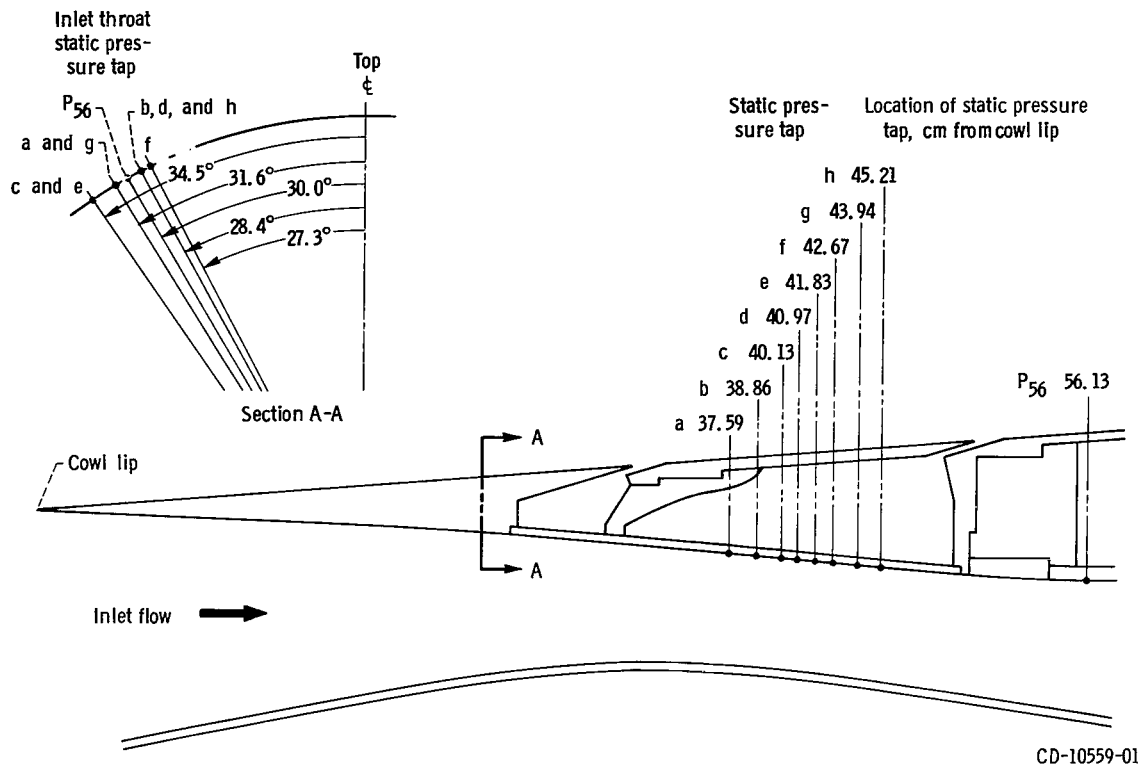


Figure 3. - Locations of Inlet throat static pressure taps used with normal shock sensor.

region from 37.59 to 45.21 centimeters from the cowl lip. The taps were closely coupled to dc strain-gage-type electronic transducers of the type used with the  $P_{56}$  tap. The existence of the normal shock at a given tap was indicated by the transition of the pressure signal from a constant low (supersonic) value with little noise content to a higher (subsonic) value with greater noise content.

A shock position sensing circuit using analog and digital electronic hardware was also implemented to determine shock position. Normal shock position was determined by finding minimums in the pressure profile measured by means of the electronic pressure transducers connected to taps a to h. The sensor, described in reference 10, had a stepwise continuous output signal that was proportional to shock position. The signal was useful for determining shock position within the tap region. However, its resolution was limited to the spacing of the taps.

With the aid of the electronic normal shock sensor and by noting the value of  $P_{56}$  at the transition points of the pressure tap traces it was possible to construct the plot of  $P_{56}$  against shock position shown in figure 4. Despite the significant changes in the gain of  $P_{56}$  to shock position indicated in figure 4, the normal shock control performed satisfactorily.



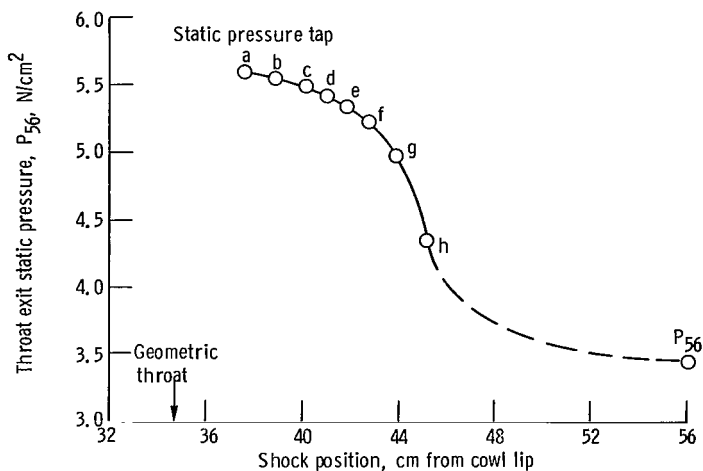


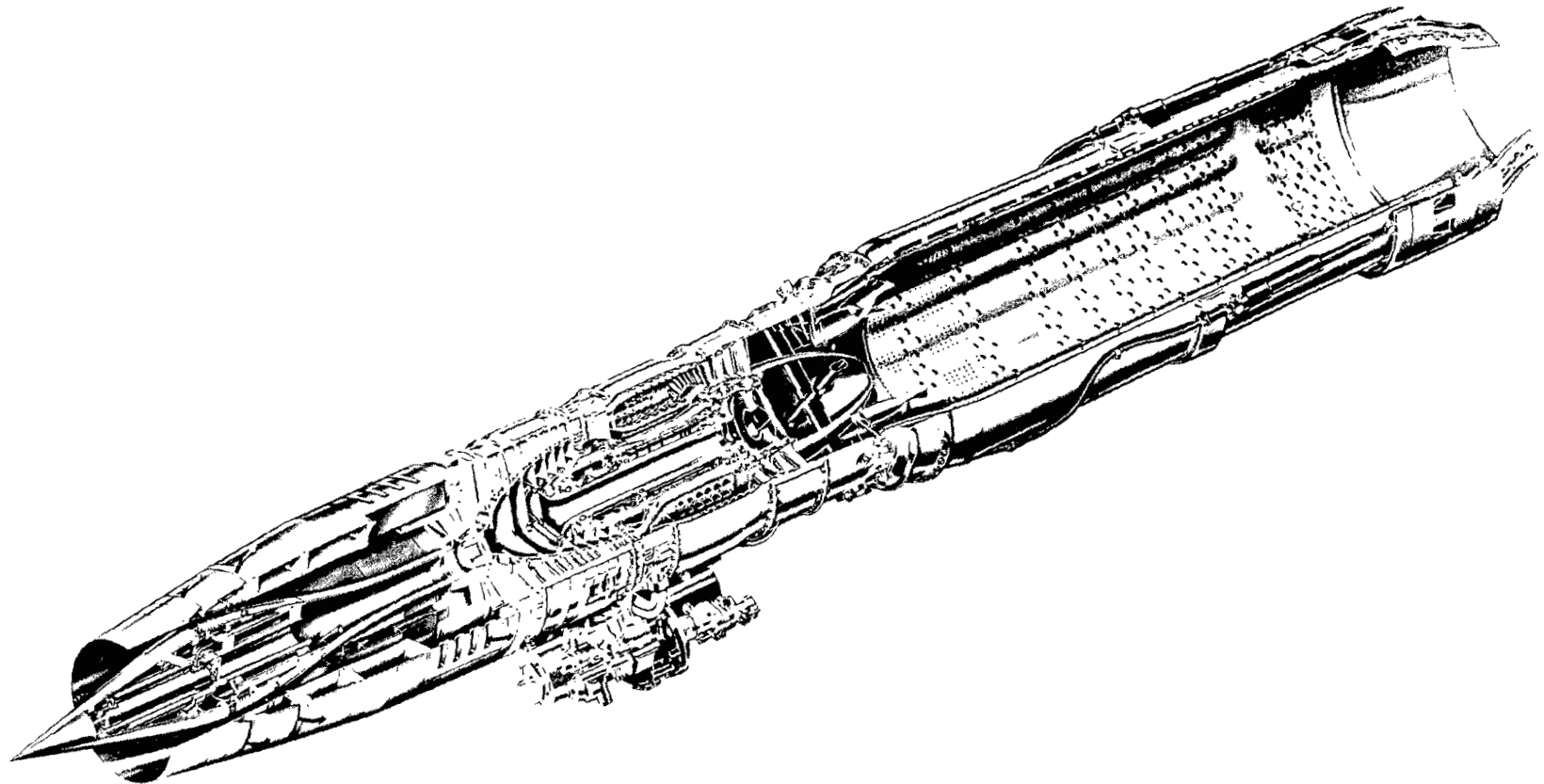
Figure 4. - Throat exit static pressure  $P_{56}$  as a function of shock position. Inlet in Mach 2.5 design configuration. Wind tunnel free stream conditions: Mach number, 2.5; total pressure, 9.5 newton per square centimeter; total temperature, 297 K; Reynolds number (based on cowl lip diam.),  $4.5 \times 10^6$ .

During tests of the coupled control, the initial normal shock position was ordinarily within the range of tap positions a to h. For these cases both the disturbance induced change in  $P_{56}$  and the corresponding shock displacement will be quoted.

## Description of Engine

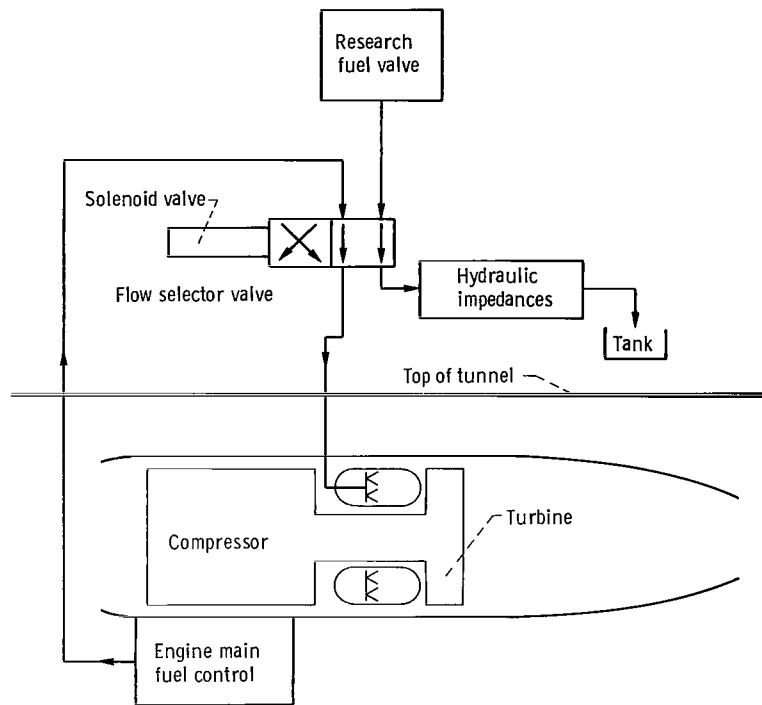
Figure 5 shows a cutaway view of the engine and inlet. The engine, A General Electric Company model J85-13, is a single-rotor afterburning turbojet engine with an eight-stage compressor, an annular combustor, and a two-stage turbine. The compressor is equipped with variable inlet guide vanes and has interstage bleed at the third, fourth, and fifth stages.

The engine's fuel control was not suited for this research investigation because it was a hydromechanical control having fixed inputs of power lever angle, speed, compressor discharge pressure, and compressor inlet temperature. Hence, there was no reasonable way to introduce into the fuel control the signals used in this investigation. Consequently, a hybrid fuel system was developed. It permitted the engine fuel flow to be obtained normally from its hydromechanical fuel control, or to be obtained from an electronically controlled research fuel valve. This hybrid fuel system is illustrated schematically in figure 6(a). Fuel flow out of the engine's main fuel control was routed out from the nacelle and tunnel test section to a flow selector valve network. Fuel was also supplied to this network through the research fuel valve. Fuel flow into the combustor could be selected to come from either the engine main fuel control or from the re-

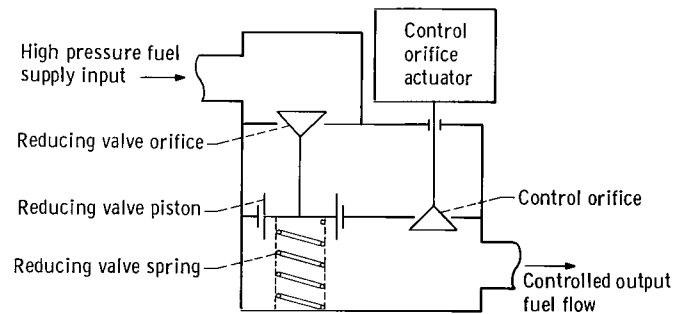


CD-10397-28

Figure 5. - Cutaway view of Inlet coupled to turbojet engine.



(a) Overall fuel system.



(b) Research fuel valve details.

Figure 6. - Engine hybrid fuel system.

search fuel valve. Simultaneously, the other flow was diverted back to a fuel tank through appropriate hydraulic impedances.

The high performance electrohydraulically controlled fuel valve which was developed at NASA Lewis Research Center is shown schematically in figure 6(b). The design and dynamic performance of this fuel valve is presented in reference 11. This reference also gives a mathematical model for the fuel valve and feed line. The valve uses a spring loaded differential reducing valve to hold a constant pressure drop across a variable area control orifice. Thus output flow rate is proportional to control orifice area independent of output pressure level. The area of the control orifice is determined by the position of a shaft which is directly actuated by an electrohydraulic servo. Thus, flow is proportional to shaft position and is measurable by an integral shaft position transducer. A typical frequency response of shaft position to fuel command for an excursion of  $\pm 1.5$  percent of full stroke is shown in figure 7.

During the test program, changes in fuel flow were inferred from a spray nozzle pressure measurement instead of being measured directly. The pressure tap was located in one of the flow divider and fuel nozzle assemblies as shown in figure 8(b). A frequency response of spray nozzle pressure was taken for a zero-to-peak command in fuel valve position of 1.5 percent of full travel. The response, shown in figure 9, exhibits a pronounced resonance at a frequency of about 15 hertz. It is believed that this resonance was caused by fuel feed system dynamics. For the wind tunnel installation

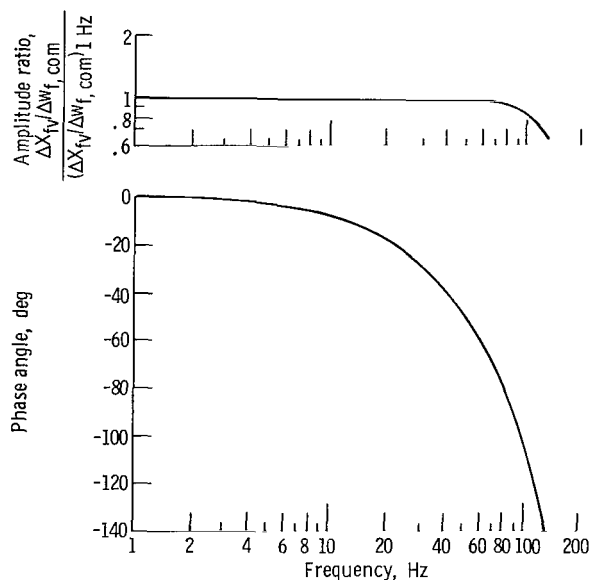
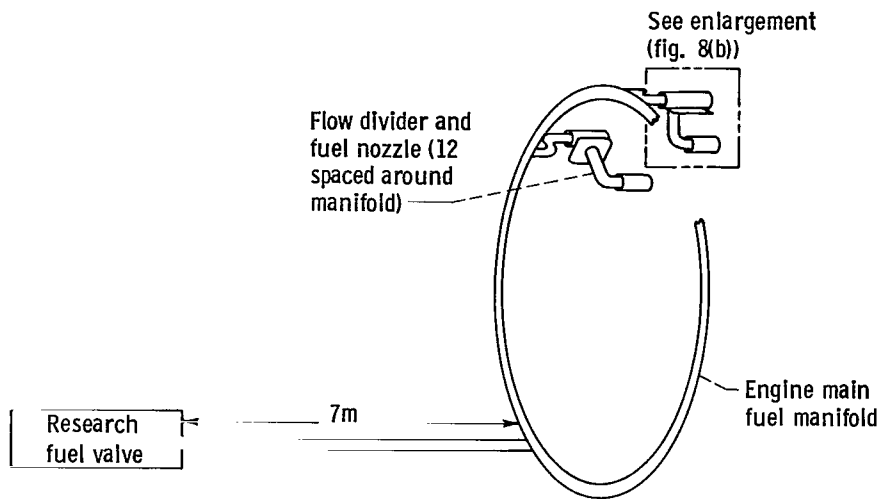
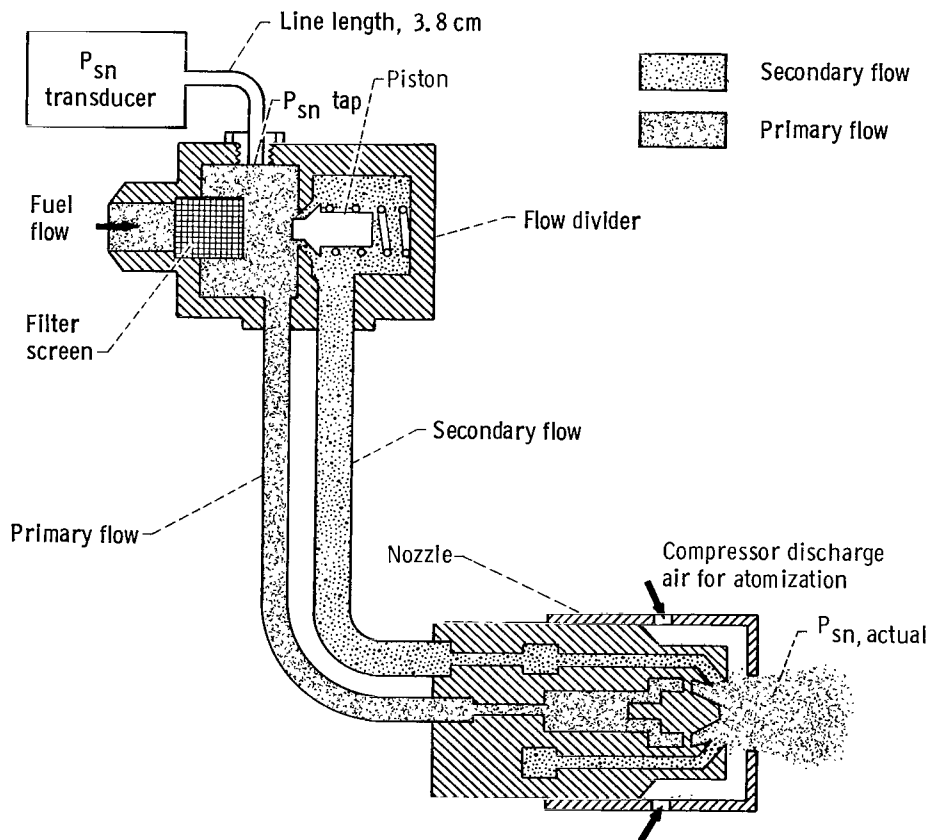


Figure 7. - Frequency response of research fuel valve position to fuel command. Valve 15 percent open at operating point. Zero-to-peak amplitude of command, 1.5 percent of full stroke.



(a) Location of flow divider and fuel nozzle.



b) Enlargement of flow divider and fuel nozzle.

Figure 8. - Schematic showing location of fuel spray nozzle pressure measurement  $P_{sn}$ .

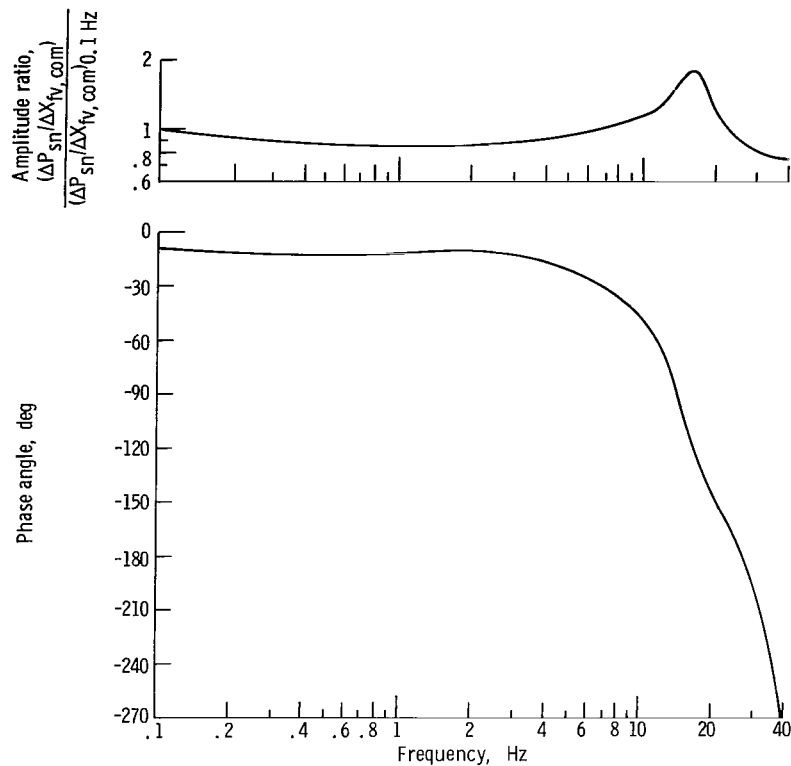


Figure 9. - Frequency response of fuel spray nozzle pressure to fuel valve command. Zero-to-peak amplitude of command, 1.5 percent of full stroke.

the fuel valve was located about 7 meters away from the fuel spray nozzles and was connected by both rigid and flexible lines.

For the data in this report, the exhaust nozzle and compressor variable geometry control systems operated according to their normal schedules. The exhaust nozzle control is primarily a function of power lever position with a turbine discharge temperature override. The data presented in this report are for a fixed power lever position and were taken below the turbine discharge temperature override, hence they are for a constant exhaust nozzle area.

The compressor variable geometry control system consists of hydraulic actuators driving a linkage mechanism which manipulates the compressor bleed doors and simultaneously moves the trailing edges of the inlet guide vanes. The normal schedule of this control system and the range of operation during this test program are shown in figure 10.

No data were taken with the afterburner in operation. To conduct a study of transients arising from operation with the afterburner, an extensive modification of the engine's afterburner fuel control would have been necessary.

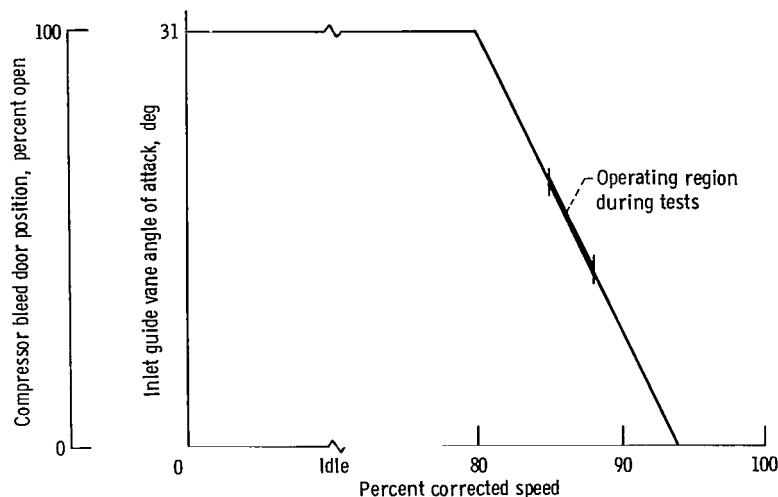


Figure 10. - Compressor variable geometry normal schedule.

## Engine Instrumentation

Engine mechanical speed was measured by an electromagnetic pickup mounted adjacent to a spur gear driven by the engine gear box. The pulse output from the pickup was converted to a dc signal by a frequency to dc converter. The response of the speed measuring circuit was characterized by a 1-millisecond time constant for a 5 percent step change in speed. For purposes of this program the speed sensor is assumed to be instantaneous.

As was discussed earlier, engine spray nozzle pressure  $P_{sn}$  was used as an indicator of the engine's fuel flow response to changes in speed command. The spray nozzle pressure tap (see fig. 8(b)) was closely coupled to a dc strain-gage-type pressure transducer. No experimental frequency response of  $P_{sn, actual}$  (see fig. 8(b)) to  $P_{sn}$  was taken. However, theoretical calculations showed the response to be within 0 to 3 decibels out to 90 hertz.

## Control Implementation and Test Procedure

A schematic of the experimental setup is shown in figure 11. The normal shock and engine speed controllers and their coupling were programmed on a 10-volt desk top analog computer located in the wind tunnel control room. The computer was used to close the normal shock and engine speed control loops. Engine startup and shutdown was accomplished by using the J85-13 fuel control.

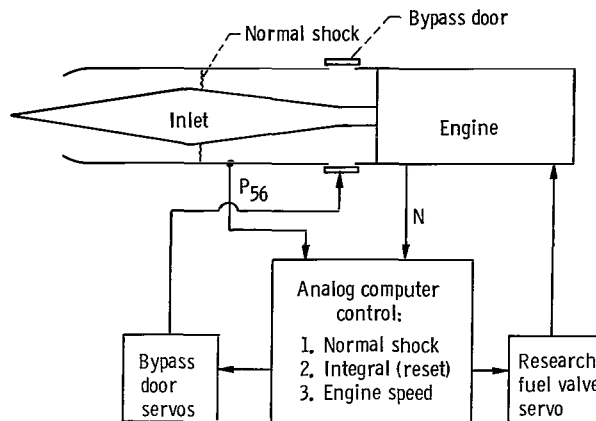


Figure 11. - Schematic showing wind tunnel test setup of inlet, engine, and controls.

Frequency responses of the normal shock control feedback variable  $P_{56}$  to diffuser exit airflow disturbances were taken with and without the normal shock control loop closed. Open- and closed-loop frequency responses of speed to speed command were also taken. The cross-coupled control was tested by introducing step disturbances in diffuser exit corrected airflow. Since the individual controllers had all electronic inputs, command and disturbance signals could easily be introduced at the appropriate summing junctions on the computer.

Frequency response data were obtained using a sweep frequency technique. This technique, described in reference 12, was used in preference to taking data at discrete frequencies primarily because it resulted in considerable time savings. The sweep rate was 1 decade per minute over the range of 1 to 140 hertz.

## DEVELOPMENT OF COUPLED INLET-ENGINE CONTROL

A block diagram of the coupled inlet-engine control system is shown in figure 12. The control system consists of two separate control loops - an inlet normal shock control loop, shown by the dashed line, and an engine speed control loop, shown by the solid line. The two loops are interconnected by an integral action controller and a limiter as indicated by the dash-dot line. The effect of diffuser exit total pressure on the engine is indicated by the loop shown as a dash-dot-dot line.

The coupled inlet-engine control was developed by first selecting and tuning the separate normal shock and speed controllers. The coupling necessary to give the desired control action was then determined. Test results are presented for the individual control loops as well as the coupled control system.



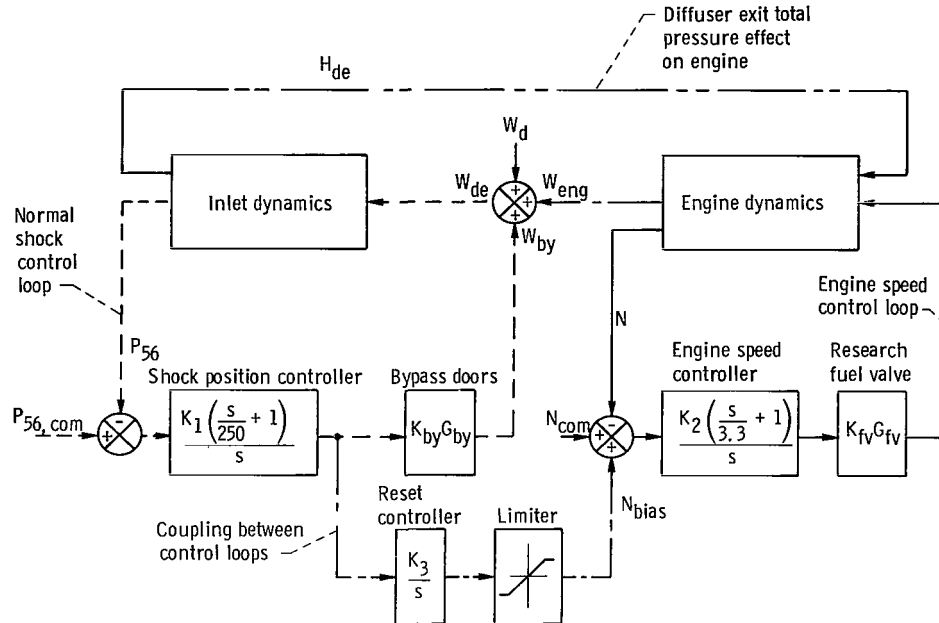


Figure 12. - Schematic showing normal shock control loop, engine speed control loop, coupling between control loops, and diffuser exit total pressure effect on engine.

## Normal Shock Controller

An analytical and experimental investigation of normal shock controls for this inlet had been conducted previous to this test program. Various types of high response controllers using electronic compensation and one or two feedback loops had been evaluated and are reported in reference 2. The normal shock controls of reference 2 used the throat exit static pressure ( $P_{56}$ , fig. 3) as the primary feedback variable and overboard bypass door area as the manipulated variable. It is recognized that, under flight conditions,  $P_{56}$  by itself would not suffice as a feedback variable. Corrections and/or biases might be required for changes in variables such as altitude, flight Mach number, and aircraft attitude. These effects were not evaluated during this program because wind tunnel conditions remained constant and only disturbances in diffuser exit airflow were used to test the control.

The normal shock control that was selected for this investigation used a single feedback loop with a proportional-plus-integral controller. It is represented by the dashed line of figure 12. This control was chosen because it was shown in reference 2 to give good normal shock control in the presence of downstream airflow disturbances. At the same time it is simpler than the two-loop control of reference 2 which gave somewhat better performance. The error between the measured and commanded values of  $P_{56}$  is transmitted to the bypass door servos through the shock position controller. The

controller gain was adjusted to give the best performance for the inlet configuration used during this investigation. The performance is indicated in figure 13 which shows the frequency responses of  $P_{56}$  to a bypass door airflow disturbance with and without the normal shock loop closed. The dc zero-to-peak amplitude of the disturbance was approximately 1.5 percent of total inlet airflow and resulted in a zero-to-peak shock displacement of about 3.8 centimeters without control. The ordinate of figure 13 is the ratio of the disturbance induced pressure change  $\Delta P_{56}$  to the airflow disturbance  $\Delta W_d$ . The amplitude ratio has been normalized at each frequency by dividing by the 1-hertz, open-loop value of the ratio. Therefore, figure 13 indicates that the normal shock control gave reduced shock motion relative to the open loop out to a frequency of 12 hertz.

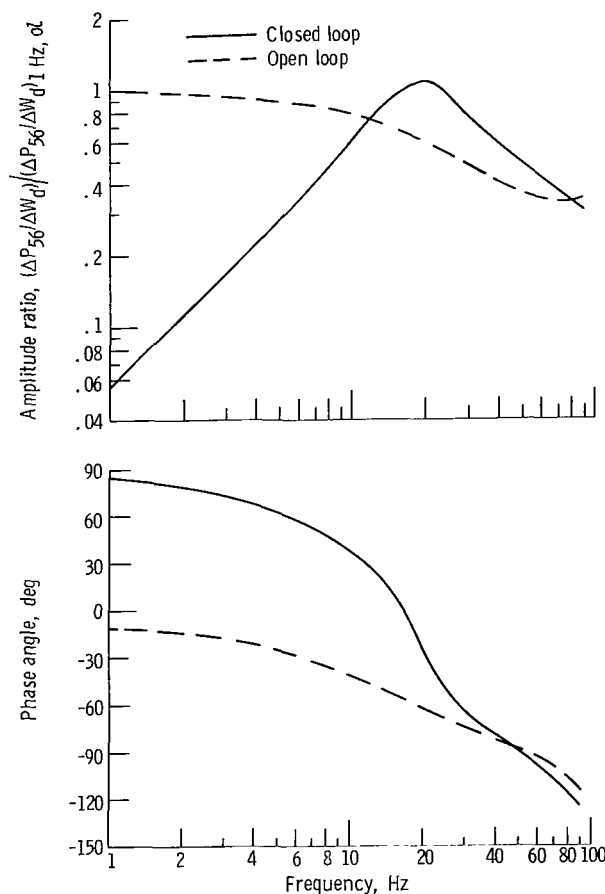


Figure 13. - Open- and closed-loop frequency responses of throat exit static pressure to diffuser exit (bypass door) airflow disturbance. Zero-to-peak amplitude of disturbance, 1.3 percent of total inlet airflow.

## Engine Speed Controller

The speed control loop is shown by the solid line in figure 12. The error in engine speed is transmitted to the research fuel valve servo through the controller. A proportional-plus-integral speed controller was chosen because it gives zero steady-state error for a constant command value due to the integral action. The speed loop was first investigated analytically with the aid of the multistage compressor analog computer simulation, described in reference 13. By using the simulation it was possible to obtain an approximate speed controller gain  $K_2$  which was later adjusted during the experimental investigation.

The experimental open- and closed-loop frequency responses of engine speed to speed command are shown in figure 14. The open-loop response does not include the controller dynamics. However, both responses include the fuel feed system dynamics.

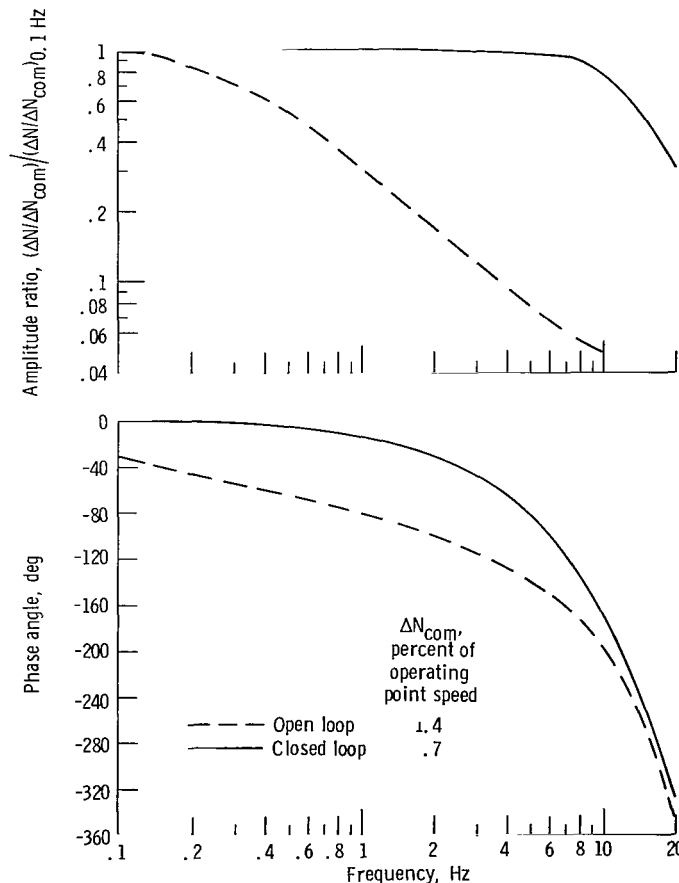


Figure 14. - Open- and closed-loop frequency responses of engine speed to speed command.

The zero-to-peak amplitude of the speed command for the open-loop test was about 200 rpm (mechanical) or approximately 1.4 percent of the operating point mechanical speed. The amplitude and phase data of figure 14 indicate that the open-loop response has the characteristics of a first order lag with a corner frequency at about 0.3 hertz. The zero-to-peak amplitude of the speed command for the closed loop test was about 100 rpm or 0.7 percent of the operating point mechanical speed. The closed-loop response is seen to be flat within 0 to -3 decibels out to a frequency of about 11 hertz. This is a considerable improvement over the open-loop response.

## Coupled Inlet-Engine Control System

The basic objective of the control was to maintain constant normal shock position while operating the overboard bypass doors at a position for most efficient propulsion system operation. The high response bypass doors initially compensate for disturbances. Then engine speed (airflow) is traded for bypass door area (airflow) to minimize overboard bypass drag. The desired control action is achieved by coupling the normal shock and speed loops by an integral controller as shown by the dash-dot line in figure 12. As can be seen from figure 12, the output of the shock position controller is transmitted as an actuating signal to the bypass door servos and as a bias in speed command  $N_{bias}$  to the speed loop. The output of the integral controller ( $N_{bias}$  signal) was limited. This limit could represent the maximum allowable change in engine speed from the cruise condition value. The limiting action could also be varied to demonstrate the capability of the coupled control to return the propulsion system to any desired operating condition.

Control action. - The control action of the coupled control can be illustrated with the aid of figure 15. It shows overboard bypass door area plotted against engine mechanical speed. The control action usually takes place in the general direction of the arrows, as shown in figure 15, but not necessarily along the arrows. The control system response to a step decrease in diffuser exit corrected airflow will be considered first. The propulsion system is initially at the operating point condition denoted as point 1 on figure 15. A decrease in  $W_d$  causes a forward motion of the normal shock resulting in higher inlet pressure recovery. The resulting increase in  $P_{56}$  causes the overboard bypass doors to react rapidly, increasing  $W_{by}$  as indicated by point 2 on the diagram. The output of the shock position controller is then integrated by the reset controller producing an increase in the engine speed biasing signal and consequently an increase in engine speed. This second action is slower due to the choice of integrator gain. As engine speed increases, the bypass doors are simultaneously closed due to the action of the shock position loop. Finally, the doors reach their initial operating position as indicated by point 3 on the diagram.

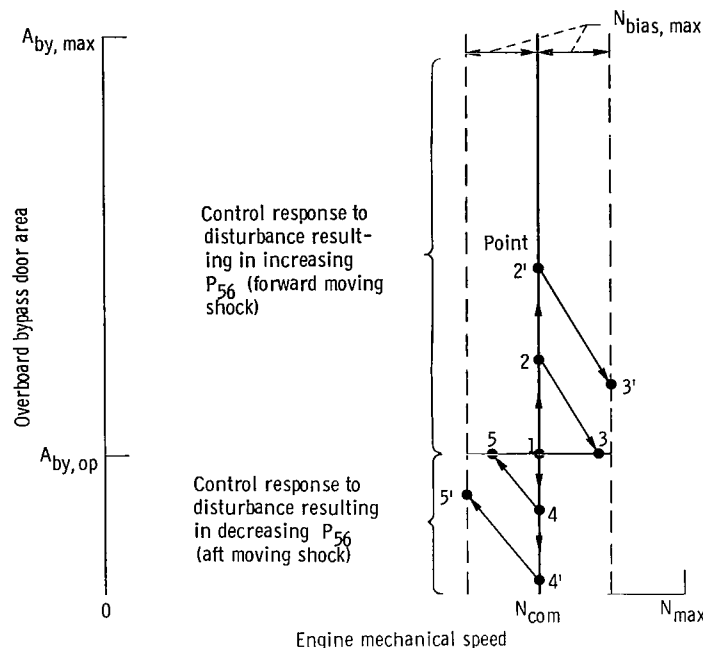


Figure 15. - Illustration of cross-coupled control action in response to disturbance in diffuser exit airflow.

If a larger airflow disturbance occurred, a larger than desired change in engine speed might be required to bring the doors back to their operating point. In that case the engine speed bias signal could be limited. An example of such a case is illustrated in figure 15 by the path 1, 2', 3'. The system would reach equilibrium at point 3' where the drag would be slightly greater than at point 3.

The coupled control action for a step increase in diffuser exit airflow (aft moving shock disturbance) depends on the initial operating position of the bypass doors. The cases where the doors are initially far enough open so that they can compensate for the disturbance are indicated by the paths 1, 4, 5 and 1, 4', 5'. These cases are equivalent to paths 1, 2, 3 and 1, 2', 3' except that the changes in bypass door area and engine speed have the opposite sign.

A different response will result when the bypass doors are initially at the closed position, which would probably be the case during a cruise condition. When the bypass doors are initially closed, the normal shock control cannot react to a disturbance which causes a shock displacement in the aft direction. This has the same effect as opening the feedback path of the normal shock control loop and results in different coupled control loop dynamics. The consequences of this will be discussed and illustrated when test results are presented.

Coupled loop dynamics. - Although the coupled control system will generally react in the manner described previously, its dynamic response will depend on the action of the

individual speed and shock position loops and on the manner in which they are interconnected. To gain an understanding of the phenomena involved it is helpful to rearrange the block diagram of figure 12 to show the individual control loops and their interconnection.

Both the engine dynamics block and the inlet dynamics block of figure 12 had dual outputs. The engine dynamics block represented by  $K_{\text{eng}}G_{\text{eng}}$  in figure 16(a), has engine speed as its only output. The response of engine corrected airflow to speed is assumed to be a pure gain and is represented in figure 16(a) by the block  $K_{\text{ca}}$ . Engine speed is fed back to the speed summing junction through the speed sensor gain  $K_v$ . The inlet dynamics block of figure 12 is represented by the block  $K_1G_1$  in figure 16(a). The effect of diffuser exit total pressure on engine speed and airflow, shown by the dash-dot-dot loop in figure 12, is neglected in figure 16(a). This effect is certainly small since deviations in shock position are small and of short duration when the normal shock control is operating normally.

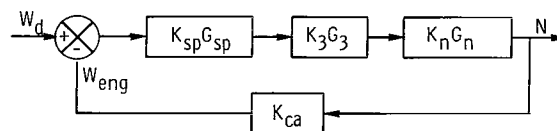
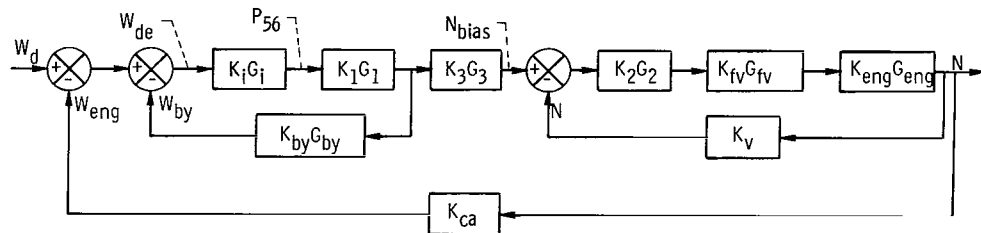


Figure 16. - Block diagrams of cross-coupled inlet-engine control system rearranged and simplified to show transfer functions between engine speed and diffuser exit corrected airflow.  $G_1 = (s/250 + 1)/s$ ;  $G_2 = (s/3.3 + 1)/s$ ;  $G_3 = 1/s$ .

is assumed to remain constant it has not been shown between the  $K_i G_i$  and the  $K_1 G_1$  blocks.  $K_{by} G_{by}$  is used in both figures 16(a) and 12 to represent the transfer function between bypass door airflow and the input command voltage to the control door servos. It represents the series combination of the door servos' closed-loop transfer function followed by the airflow-to-position transfer function of the door valves. Since the doors were frequently operated in a region where the airflow-to-position gain was low or even zero (when the doors were closed), it can be seen that a wide variation in values of  $K_{by}$  can be expected.

The diagram in figure 16(a) can be further reduced to that in figure 16(b) where  $K_{sp} G_{sp}$  and  $K_n G_n$  represent the closed-loop transfer functions of the shock position and engine speed loops. The values of  $K_{sp} G_{sp}$  and  $K_n G_n$  can be written in terms of the basic transfer functions of the blocks. Thus,

$$K_{sp} G_{sp} = \frac{K_i K_1 G_i G_1}{1 + K_i K_1 K_{by} G_i G_1 G_{by}} \quad (1)$$

$$K_n G_n = \frac{K_2 K_{fv} K_{eng} G_2 G_{fv} G_{eng}}{1 + K_2 K_{fv} K_{eng} K_v G_2 G_{fv} G_{eng}} \quad (2)$$

By using the nomenclature of figure 16(b) the closed-loop transfer function of the coupled loop is given by

$$\frac{N}{W_d}(s) = \frac{K_{sp} K_3 K_n G_{sp} G_3 G_n}{1 + K_{ca} K_{sp} K_3 K_n G_{sp} G_3 G_n} \quad (3)$$

Thus the characteristic equation which determines the stability of the coupled loop is

$$1 + K_{ca} K_{sp} K_3 K_n G_{sp} G_3 G_n = 0 \quad (4)$$

Once the speed and bypass door loops are set, the parameters which could change to affect stability are  $K_3$ , the integrator gain, and  $K_{sp} G_{sp}$ , which changes with bypass door position.

For frequencies of about 10 hertz or less, where the loop gains of the  $K_{sp} G_{sp}$  and  $K_n G_n$  loops are high ( $|K_i K_1 K_{by} G_i G_1 G_{by}| \gg 1$  and  $|K_2 K_{fv} K_{eng} K_v G_2 G_{fv} G_{eng}| \gg 1$ ) and where the bypass door frequency response is flat ( $G_{by} = 1$ ), equations (1) and (2) reduce to

$$K_{sp} G_{sp} = \frac{1}{K_{by}} \quad (5)$$

and

$$K_n G_n = \frac{1}{K_v} \quad (6)$$

Substituting equations (5) and (6) and  $1/s$  for  $G_3$  into equation (3) gives

$$\frac{N}{W_d}(s) = \frac{\frac{1}{K_{ca}}}{1 + \left( \frac{K_v K_{by}}{K_{ca} K_3} \right) s} \quad (7)$$

Thus equation (7) indicates that the closed-loop response of the coupled control is a first order lag. In some cases, as will be seen in the data section, the response of speed to diffuser exit airflow exhibited this first order lag characteristic. However, when the doors were closed or at a position where the gain of airflow to position was low, a resonant type of response was exhibited. This is not unexpected since the assumptions made to derive equation (7) were no longer valid.

## RESULTS AND DISCUSSION

During the test program, the following effects on the performance of the coupled control system were studied: (1) the variation in the gain of bypass door flow to position  $K_{by}$ , (2) the gain of the integral reset controller  $K_3$ , and (3) the allowable change in the engine speed command bias signal  $N_{bias, max}$ . The experimental results that are presented demonstrate the cross-coupled control's response when the propulsion system was disturbed from a steady-state operating condition.

### Effect of Bypass Door Gain $K_{by}$

The change in the control bypass door gain  $K_{by}$  was due to the nonlinear variation of bypass door area (and thus airflow) with position as shown in figure 17. As noted in



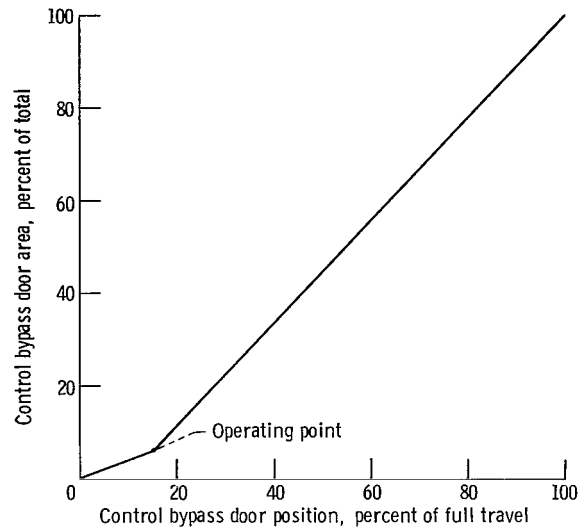


Figure 17. - Control bypass door area as a function of position.

figure 17 the area-to-position curve has two slopes or values of gain - a low gain when the doors are at a position less than 15 percent of full travel and a higher gain when the doors are farther opened. When the control bypass doors are fully open or closed,  $K_{by}$  is zero for forward and aft disturbance induced shock motions, respectively. The effect of the two nonzero gains on coupled control performance were demonstrated by disturbing the inlet with opposite polarity steps in diffuser exit corrected airflow. For those cases the control doors were initially at the operating point indicated in figure 17. The effect of zero  $K_{by}$  was demonstrated by electronically preventing control door servo inputs which would cause the doors to move in the closed direction. The operating point was the same as the one used previously and the disturbance was a step increase in diffuser exit airflow.

Effect of nonzero bypass airflow-to-position gain  $K_{by}$ . - The effect of changes in  $K_{by}$  due to step disturbances in inlet exit airflow of either polarity is shown in figures 18 and 19. The same reset gain  $K_3$  was used in both cases and was considered to be the design value. The traces shown in these figures indicate the change of each variable from its initial (operating point) value. Deflections in the upward direction indicate an increase in the magnitude of the variable. Initial inlet and engine conditions are listed in each figure. All figures showing transient responses have the same format.

Figure 18 shows the case of a step decrease in diffuser exit airflow of about 1 percent of total inlet airflow. The control doors were initially at their operating point (point 1, fig. 18) which corresponds to point 1 in figure 15. The normal shock control reacts rapidly (less than a 10 msec delay) and opens the bypass doors to point 2 (cor-

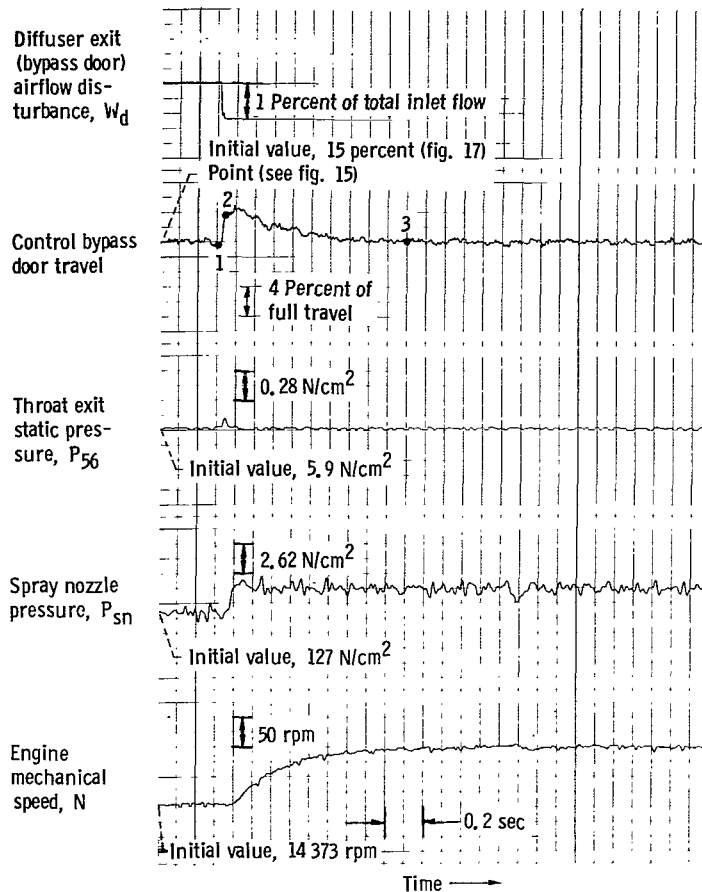


Figure 18. - Response of coupled control system to step decrease in diffuser exit corrected airflow. Initial inlet conditions: shock position, upstream of static pressure tap a (see fig. 3); total pressure recovery, 0.89. Initial engine conditions: percent corrected speed, 86.1; compressor total pressure ratio, 4.01. Reset gain  $K_3/K_{3,des}$ , 1.0.

responding to point 2 of fig. 15) holding  $P_{56}$  almost constant.  $P_{56}$  shows a momentary increase of only 0.08 newton per square centimeter. The normal shock displacement could not be determined because it was initially positioned forward of the region in which  $P_{56}$  was known as a function of shock position. The normal shock controller output acting through the integral reset controller resulted in an increase in the speed bias command  $N_{bias}$ . The response of the speed control loop to the change in  $N_{bias}$  was first indicated by the increase in fuel spray nozzle pressure, approximately 60 milliseconds after the control doors began to move. After a further time delay of about 20 milliseconds, engine speed began to increase, responding to the increase in fuel flow. As engine speed increased, the control bypass doors were simultaneously returned to their initial position. The net change in engine speed was approximately 100 rpm or 0.7 percent of its initial operating mechanical speed. The final engine operating condi-

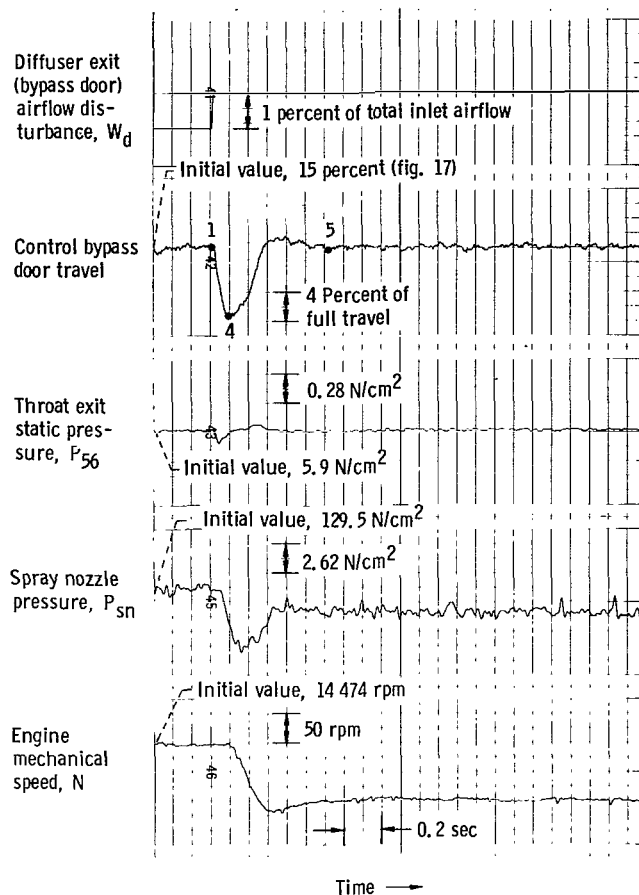


Figure 19. - Response of coupled control system to step increase in diffuser exit corrected airflow. Initial inlet conditions: shock position, upstream of static pressure tap a (see fig. 3); total pressure recovery, 0.89. Initial engine conditions: percent corrected speed, 86.7; compressor total pressure ratio, 4.12. Reset gain  $K_3/K_{3, des}$  1.0.

tion was not significantly different than its initial condition and the inlet was returned to its initial condition point 3 (corresponding to point 3, fig. 15) in about 1.0 second. Meanwhile shock position was held constant.

The transient data of figure 18 indicate that in this case the closed-loop system of figure 16(b) behaved approximately as a first order system. The time at which speed changed by 63.3 percent of the change in  $N_{bias}$  is equivalent to one time constant and can be found from figure 18 to be approximately 250 milliseconds. This would correspond to a closed-loop frequency response having a corner frequency at approximately 4 radians per second or 0.64 hertz. Increasing the gain  $K_3$  of the reset controller could be expected to shorten this time constant as indicated by equation (7).

The case of the step increase disturbance in diffuser exit airflow is shown in figure 19. The magnitude of the disturbance was the same as for the case of figure 18 and

the sequence of events is the same except that changes in control bypass door airflow and engine speed have the opposite sign. Points 1, 4, and 5 correspond to points 1, 4, and 5 of figure 15.

The major difference between the coupled control responses of figures 18 and 19 is that engine speed responds much faster in the latter case. The engine speed trace of figure 19 (which also exhibits the time delay of about 80 msec found in fig. 18) shows an overshoot of about 20 percent. After speed begins to decrease, it reaches 90 percent of the change in  $N_{bias}$  in 150 milliseconds and settles to within 5 percent of the change in  $N_{bias}$  in about 350 milliseconds. This could be characteristic of a second order system with a damping ratio slightly less than 0.5 and an undamped natural frequency of about 14 radians per second or 2.2 hertz.

It is recalled that the first order lag relation between engine speed and diffuser exit corrected airflow (eq. (7)) depended on  $K_{by}$  being high. For the case of figure 19, however, the control bypass doors were operating in the low gain region of figure 17. Thus, equation (7) is not applicable to the case of figure 19 because assumptions used to derive it were violated. It can be seen from equation (1) that  $|K_{sp}G_{sp}|$  increases as  $K_{by}$  decreases. The change in  $|K_{sp}G_{sp}|$  in turn affects the loop gain of the coupled control. This change in gain plus the inclusion of higher order dynamic terms is the main reason for the change in stability between the transients of figures 18 and 19. Such changes in stability are not a generic limitation in this kind of control. A nonlinear element at the input to the reset integrator could be used to maintain nearly constant outer loop gain. Electronically this could be done with a diode function generator. Mechanically it could be done with a cam. Such a gain compensating feature was not implemented in this program.

Effect of zero bypass airflow-to-position gain  $K_{by}$ . - The coupled control's response to a step increase in diffuser exit airflow with the control bypass doors initially at the simulated closed position is shown in figure 20. Since the control doors were electronically limited from closing ( $K_{by} = 0$ ), they could not respond to the disturbance. This is equivalent to eliminating feedback from the shock position loop. The decrease in  $P_{56}$  was approximately two times greater than that for the case of figure 19. The aft shock displacement for the case of figure 20 was also greater. The increase in gain and change in dynamics of the coupled control loop, due to the elimination of feedback from the shock position control loop, resulted in a response that was more unstable than that of figure 19. For the case of figure 20, speed overshoot the change in  $N_{bias}$  by about 350 percent. It is inferred from the  $P_{56}$  trace of figure 20 that the normal shock reached a maximum downstream position (about 2.2 cm from the operating point) before engine speed began to decrease. The decrease in engine speed caused the shock to move upstream. The normal shock overshoot its initial position in the upstream direction as indicated by the 0.48 newton per square centimeter increase in  $P_{56}$  above its initial

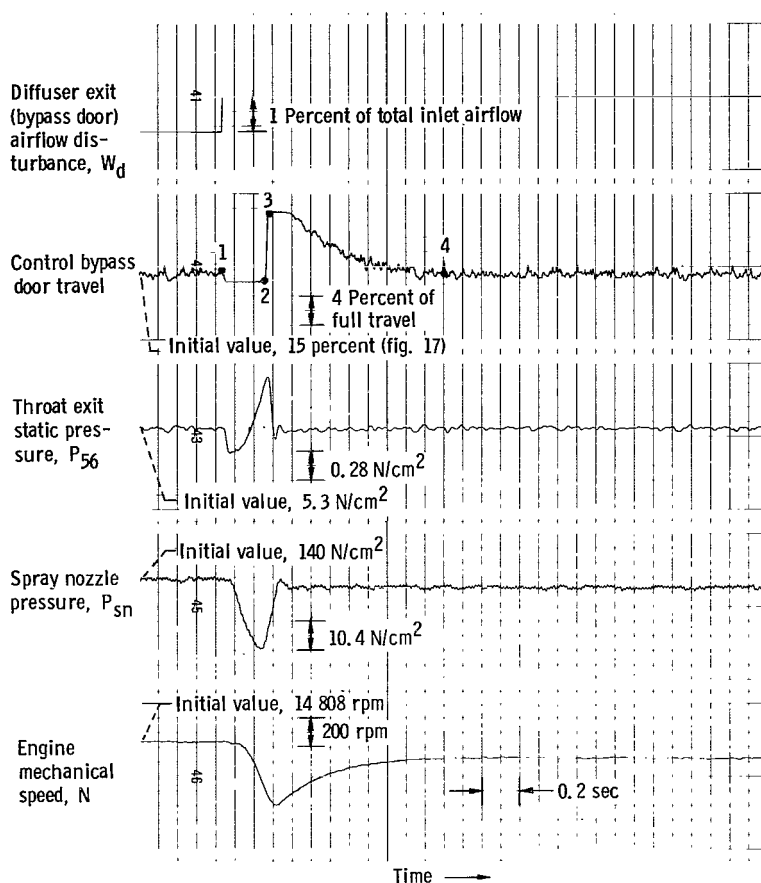


Figure 20. - Response of coupled control system to step increase in diffuser exit corrected airflow. Control bypass doors limited from moving in closed direction at operating point. Initial inlet conditions: shock position, 42 centimeters from cowl lip; total pressure recovery, 0.87. Initial engine conditions: percent corrected speed, 87.6; compressor total pressure ratio, 4.45. Reset gain  $K_3/K_{3, des}$ , 1.0.

value. The shock moved up into the region where its position could not be determined. The upstream shock excursion was thus greater than 4.4 centimeters from its initial position. The normal shock control did not begin to correct for the forward moving shock until 80 milliseconds after the shock had passed its operating point.

The reason for the delay in correcting for the forward moving shock can be explained by referring to figure 12. There are two contributions to the normal shock controller output - the proportional part and the integral part. For the sake of argument assume that both contributions were initially zero. When the normal shock moved from a position downstream to a position upstream of the operating point, the proportional contribution to the controller output changed sign immediately. However, the integrator's contribution did not change sign until it had first integrated back to zero. This resulted in the shock overshooting its operating point in the upstream direction. Thus the shock

controller's net output did not change sign until the proportional positive contribution exceeded the integrator's negative contribution. Thus the shock had to move forward of its operating point. For the test of figure 20, therefore, the shock controller output did not change sign until 80 milliseconds after the shock passed its operating point. Once the shock controller output changed sign, requiring the bypass doors to open, feedback was restored to the shock control loop and the shock was returned to its operating point. The sign of the  $N_{bias}$  signal was also reversed requiring the engine to speed up so that the bypass doors could be closed to the initial position (which occurs in going from point 3 to 4). After feedback was restored to the shock control loop, the dynamics and gain of the coupled control loop changed so that engine speed responded stably, as can be seen in figure 20. The control action for this case is demonstrated graphically in figure 21. Points 1, 2, 3, and 4 in figures 20 and 21 are equivalent.

The overshoot of the shock in the upstream direction is undesirable and should be eliminated because it could result in an inlet unstart. One method would be to prevent inputs to the normal shock controller integrator due to aft shock displacements as long as the bypass doors are at the closed position. Thus the output of the normal shock controller would be directly proportional to the error in  $P_{56}$  as long as the shock is downstream of its operating point and, assuming zero initial conditions, would change to the opposite polarity when the shock passes over its operating point in the upstream direction. This solution would also help to reduce the engine speed overshoot exhibited in figure 20.

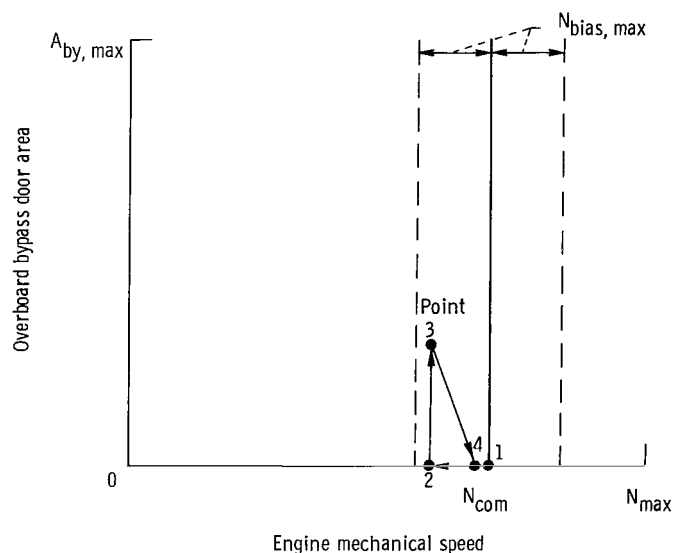


Figure 21. - Illustration of coupled control response to decrease in diffuser exit airflow with control bypass doors limited from closing at operating point.

For the case when the bypass doors are initially closed and the inlet is subjected to an aft disturbance induced shock displacement, the coupled control system allows zero steady-state error in shock position. The uncoupled controls do not. This is an important advantage of the coupled control system because downstream shock displacements generally increase distortion and decrease total pressure recovery at the diffuser exit. These conditions reduce propulsion system efficiency and increase the possibility of a compressor stall.

### Effect of Reset Integral Gain

The effect on the cross-coupled control performance due to a decrease in the integrator gain  $K_3$  is shown in figure 22. The case shown is for a step increase disturb-

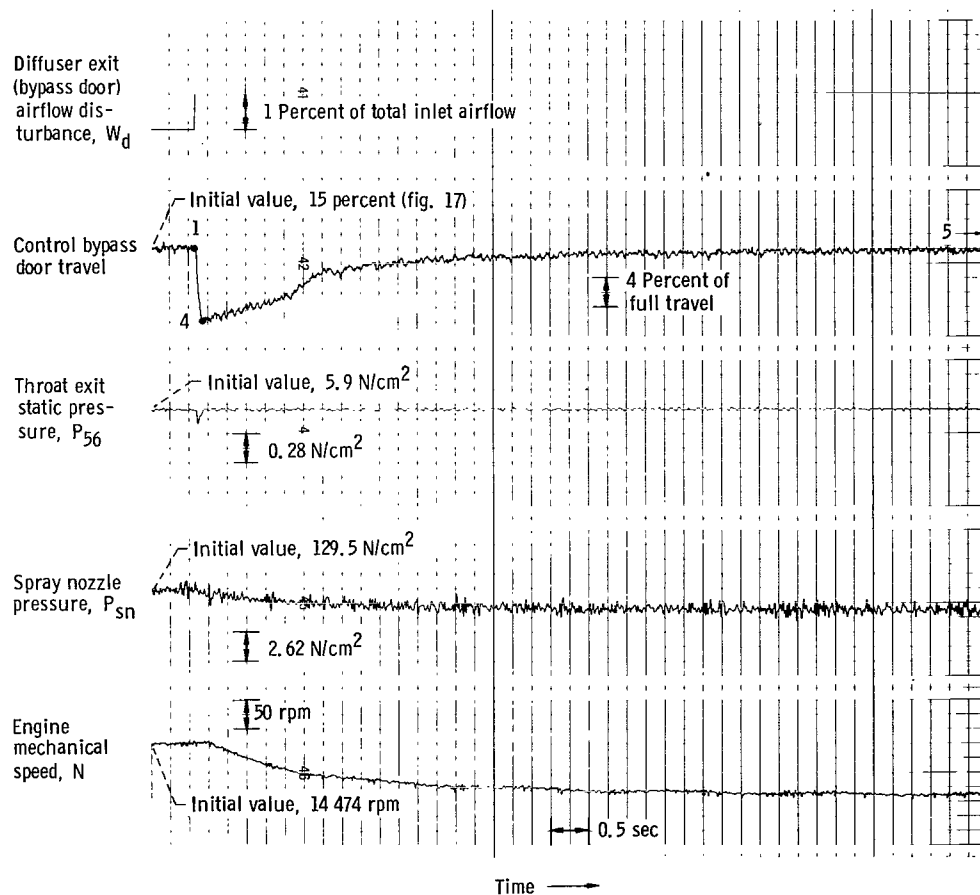


Figure 22. - Response of coupled control system to a step increase in diffuser exit corrected airflow. Initial inlet conditions; shock position, upstream of static pressure tap a (see fig. 3); total pressure recovery, 0.89. Initial engine conditions; percent corrected speed, 86.7; compressor total pressure ratio, 4.12. Reduced value of reset gain  $K_3/K_{3,des}$ , 0.067.

ance in inlet exit airflow having the same magnitude as that shown in figure 19. The reset gain of figure 22 was one-fifteenth that for the case shown in figure 19. As expected, the lower gain resulted in a much slower response of engine speed to the step disturbance in diffuser exit airflow. After engine speed started to decrease, it changed by 63.3 percent of the change in  $N_{bias}$  in about 2.25 seconds.

## Effect of Limiting Change in Engine Speed Bias Signal

A case where the change in  $N_{bias}$  command was limited is shown in figure 23. The disturbance and initial inlet and engine operating conditions were approximately the

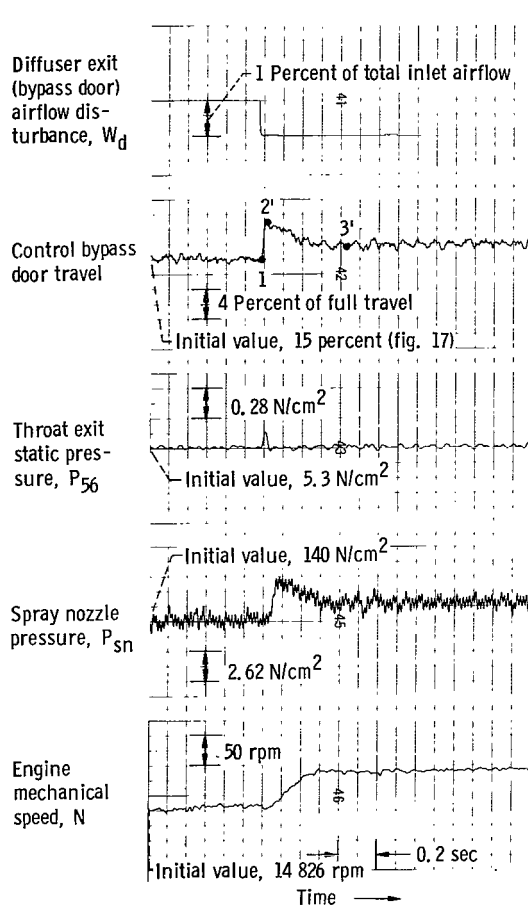


Figure 23. - Coupled control response to step decrease in diffuser exit corrected airflow. Change in speed command from reset action limited. Initial inlet conditions: shock position, 42 centimeters from cowl lip; total pressure recovery, 0.87. Initial engine conditions: percent corrected speed, 87.8; compressor total pressure ratio, 4.45. Reset gain  $K_3/K_{3,des}$  1.0.



same as those shown in figure 18. Since the allowed change in engine speed did not result in a change in engine airflow equal to that of the disturbance, the control bypass doors did not return to their initial position. The control action corresponds to path 1, 2', 3' shown in figure 15. Limiting the change in  $N_{bias}$  caused no special problems in the operation of the coupled control system. The limiting action primarily demonstrates the capability of the coupled control to return the propulsion system to any desired operating condition.

## SUMMARY OF RESULTS

A supersonic inlet-turbojet engine cross-coupled control system was described which used the inlet overboard bypass doors and engine speed as the primary and secondary means, respectively, for controlling shock position. The error in shock position is detected and results in the initial corrective action by the fast inlet bypass door control loop to maintain the desired normal shock position. The error in bypass position results in a second, relatively slow corrective action by the engine speed loop, which changes engine speed until the error in bypass door position is nulled, while maintaining a fixed normal shock position. One advantage of this system is that the bypass doors can be maintained at the most advantageous (low drag) position except for momentary corrections. There is also an advantage for the case when the bypass doors are initially closed and a disturbance causes the normal shock to move downstream. The coupled control system would give zero steady-state error in shock position whereas the uncoupled controls would not.

The coupled control system was demonstrated to work satisfactorily when the inlet was subjected to step disturbances in diffuser exit corrected airflow. With the proper overall loop gain the coupled control returned the bypass doors to their desired position in 1 second or less. At the same time, constant shock position was maintained except for a small momentary shock position displacement when the disturbance occurred.

Inherent changes in the shock position loop gain and dynamics due to the nonlinear variation of bypass door area with position did not seriously affect the dynamic response of the coupled control. One exception occurred when the bypass doors were limited from closing and a disturbance resulted in a downstream shock displacement. The bypass doors could not correct for the disturbance which is equivalent to having no feedback in the shock position control loop. This caused the engine to overshoot its required decrease in speed by 350 percent. The variation in coupled control loop gain and dynamics due to gain changes and limiting of the bypass doors could be corrected by refinements in the shock position controller.

Limiting the engine corrective action to an amount less than that required to return the bypass doors to their initial position was shown to have no detrimental effect on the coupled control action. The limit demonstrated the capability of the coupled control to return the propulsion system to any desired operating condition.

Lewis Research Center,  
National Aeronautics and Space Administration,  
Cleveland, Ohio, August 20, 1970,  
720-03.

## APPENDIX - SYMBOLS

A	area, cm <sup>2</sup>	by	overboard bypass doors
G	transfer function dynamic term	ca	refers to gain of engine corrected airflow to engine speed
H	total pressure, N/cm <sup>2</sup>		
K	gain term of transfer function	com	command or reference value
N	engine mechanical speed, rpm	d	disturbance
$\frac{100 \left( \frac{N}{\sqrt{\theta}} \right)}{16\ 500}$	percent engine corrected speed, dimensionless	de	at or near diffuser exit
P	static pressure, N/cm <sup>2</sup>	des	design or nominal value
s	Laplace operator, sec <sup>-1</sup>	eng	engine
T	total temperature, K	fv	research fuel valve
W	corrected airflow, kg/sec	i	inlet
w	actual airflow, kg/sec	max	maximum
w <sub>f</sub>	fuel flow, kg/sec	n	engine speed closed-loop control
X	position, cm	ol	open loop or uncontrolled
Δ	zero-to-peak amplitude of sinusoidal variation	op	operating point
δ	corrected total pressure, H/10.13, dimensionless	sn	fuel spray nozzle
θ	corrected total temperature, T/288.2, dimensionless	sp	normal shock position closed-loop control
Subscripts:		v	refers to gain of volts to engine speed
bias	refers to speed command bias from normal shock control loop	1	normal shock controller
		2	engine speed controller
		3	integral (reset) controller
		56	inlet throat exit station 56.13 cm aft of cowl lip

## REFERENCES

1. Koenig, Robert W.: Inlet Sensitivity Study for a Supersonic Transport. NASA TN D-3881, 1967.
2. Crosby, Michael J.; Neiner, George H.; and Cole, Gary L.: Restart and High Response Terminal Shock Control for an Axisymmetric Mixed-Compression Inlet with 60-Percent Internal Contraction. NASA TM X-1792, 1969.
3. Chun, K. S.; and Burr, R. H.: A Control System Concept and Substantiation Test for an Axisymmetric Mixed Compression Supersonic Inlet. Paper 68-581, AIAA, June 1968.
4. Martin, Arnold W.: Propulsion System Flow Stability Program (Dynamic). Part I. Summary. Rep. NA-69-870-Pt. 1, North American Rockwell Corp. (AFAPL-TR-69-113, pt. 1, DDC No. AD-866497), Feb. 1970.
5. Paulovich, Francis J.; Neiner, George H.; and Hagedorn, Ralph E.: A Supersonic Inlet-Engine Control Using Engine Speed as a Primary Variable for Controlling Normal Shock Position. NASA TN D-6021, (E-5492).
6. Cubbison, Robert W.; Meleason, Edward T.; and Johnson, David F.: Effect of Porous Bleed in a High-Performance, Axisymmetric, Mixed-Compression Inlet at Mach 2.50. NASA TM X-1692, 1968.
7. Cubbison, Robert W.; Meleason, Edward T.; and Johnson, David F.: Performance Characteristics from Mach 2.58 to 1.98 of an Axisymmetric, Mixed-Compression Inlet System with 60-Percent Internal Contraction. NASA TM X-1739, 1969.
8. Wasserbauer, Joseph F.: Dynamic Response of a Mach 2.5 Axisymmetric Inlet with Engine and Cold Pipe and Utilizing 60 Percent Supersonic Internal Area Contraction. NASA TN D-5338, 1969.
9. Zeller, John R.: Design and Analysis of a Modular Servoamplifier for Fast-Response Electrohydraulic Control Systems. NASA TN D-4898, 1968.
10. Cole, Gary L.; Neiner, George H.; and Crosby, Michael J.: Design and Performance of a Digital Electronic Normal Shock Position Sensor for Mixed-Compression Inlets. NASA TN D-5606, 1969.
11. Batterton, Peter G.; and Zeller, John R.: Dynamic Performance Analysis of a Fuel-Control Valve for Use in Airbreathing Engine Research. NASA TN D-5331, 1969.

12. Drain, Daniel I.; Bruton, William M.; and Paulovich, Francis J.: Airbreathing Propulsion System Testing Using Sweep Frequency Techniques. NASA TN D-5485, 1969.
13. Willoh, Ross, G.; and Seldner, Kurt: Multistage Compressor Simulation Applied to the Prediction of Axial Flow Instabilities. NASA TM X-1880, 1969.

NATIONAL AERONAUTICS AND SPACE ADMINISTRATION

WASHINGTON, D. C. 20546

OFFICIAL BUSINESS

FIRST CLASS MAIL



POSTAGE AND FEES PAID  
NATIONAL AERONAUTICS AND  
SPACE ADMINISTRATION

04U 001 53 51 3DS 70329 00903  
AIR FORCE WEAPONS LABORATORY /WL0L/  
KIRTLAND AFB, NEW MEXICO 87117

ATT E. LOU BOWMAN, CHIEF, TECH. LIBRARY

POSTMASTER: If Undeliverable (Section 158  
Postal Manual) Do Not Return

*"The aeronautical and space activities of the United States shall be conducted so as to contribute . . . to the expansion of human knowledge of phenomena in the atmosphere and space. The Administration shall provide for the widest practicable and appropriate dissemination of information concerning its activities and the results thereof."*

— NATIONAL AERONAUTICS AND SPACE ACT OF 1958

## NASA SCIENTIFIC AND TECHNICAL PUBLICATIONS

**TECHNICAL REPORTS:** Scientific and technical information considered important, complete, and a lasting contribution to existing knowledge.

**TECHNICAL NOTES:** Information less broad in scope but nevertheless of importance as a contribution to existing knowledge.

**TECHNICAL MEMORANDUMS:** Information receiving limited distribution because of preliminary data, security classification, or other reasons.

**CONTRACTOR REPORTS:** Scientific and technical information generated under a NASA contract or grant and considered an important contribution to existing knowledge.

**TECHNICAL TRANSLATIONS:** Information published in a foreign language considered to merit NASA distribution in English.

**SPECIAL PUBLICATIONS:** Information derived from or of value to NASA activities. Publications include conference proceedings, monographs, data compilations, handbooks, sourcebooks, and special bibliographies.

**TECHNOLOGY UTILIZATION PUBLICATIONS:** Information on technology used by NASA that may be of particular interest in commercial and other non-aerospace applications. Publications include Tech Briefs, Technology Utilization Reports and Notes, and Technology Surveys.

*Details on the availability of these publications may be obtained from:*

SCIENTIFIC AND TECHNICAL INFORMATION DIVISION  
NATIONAL AERONAUTICS AND SPACE ADMINISTRATION  
Washington, D.C. 20546